

Gravitational Lensing Effect on the Two-Point Correlation Function of Hot Spots in 21 cm fluctuations

Hiroyuki Tashiro¹, Toshifumi Futamase²

¹ *Institut d'Astrophysique Spatiale, Université Paris-Sud XI and CNR, Orsay, F-91405, (France)*

² *Astronomical Institute, Tohoku University, Sendai 980-8578, (Japan)*

23 August 2021

ABSTRACT

We investigate the weak gravitational lensing effect on the two-point correlation function of local maxima (hot spots) in the cosmic 21 cm fluctuation map. The intrinsic two-point function has a pronounced depression feature around the angular scale of $\theta \sim 40'$, which depends on the observed frequency and corresponds to the scale of the acoustic oscillation of cosmic plasma before the recombination. It is found that the weak lensing induces a large w -dependent smoothing at that scale where w is the equation of state parameter of dark energy and thus provides a useful constraints on the dark energy property combined with the depression angular scales on the two-point correlation function.

Key words: cosmology: theory – large-scale structure of universe

1 INTRODUCTION

There has been a growing interest to use the cosmic 21 cm background fluctuations for a useful tool to study the so-called dark age of the universe. The emission and absorption lines of the 21 cm spin-flip transition of neutral hydrogen produce Cosmic Microwave Background (CMB) brightness temperature fluctuations of order ± 10 mK. By scanning through redshift frequencies of 21 cm line, it is possible to observe the evolution of the neutral hydrogen density with time. Therefore, the observation of the 21 cm fluctuations is expected as a promising probe of the reionisation history (Zaldarriaga et al. 2004; McQuinn et al. 2006). In order to measure the fluctuations, there are planned low-frequency radio arrays, for example, Mileura Wide field Array¹ (MWA), Low Frequency Array² (LOFAR) and Square Kilometer Array³ (SKA). Moreover, the 21 cm cross-correlation with other observations, e.g. CMB, large scale structures and galaxies, also studied because the cross-correlation with complementary observation gives more information than their respective auto-correlations (Alvarez et al. 2006; Tashiro et al. 2008; Adshead & Furlanetto 2008; Lidz et al. 2009).

The 21 cm observations also have a potential to reveal the Universe at high redshifts before the reionisation epoch (Madau et al. 1997; Tozzi et al. 2000). The physics of the 21 cm fluctuations at high redshifts is understood better than at lower redshifts around the reionisation epoch (for a detailed review, see Lewis & Challinor 2007). The 21 cm fluctuations at high redshifts trace the matter power spectrum and are calculated in the linear theory. The observations of the acoustic oscillations in the 21 cm fluctuations are expected to be a probe of the composition and geometry of the Universe (Barkana & Loeb 2005; Mao & Wu 2008).

In addition to these primordial fluctuations, there exist secondary 21 cm fluctuations. Modification by weak gravitational lensing is considered as one of the main sources of secondary fluctuations (Mandel & Zaldarriaga 2006). The path of the emitted 21 cm photon is perturbed by weak gravitational lensing of large scale structures. Gravitational lensing modifies the primordial 21 cm fluctuations as in the context of CMB. However, in contrast to the CMB case where there is only one source plane at the last scattering surface, the redshifted 21 cm fluctuations provide excellent sources for gravitational lensing because of the existences of many different source planes.

¹ <http://www.haystack.mit.edu/array/MWA>

² <http://www.lofar.org>

³ <http://www.skatelescope.org>

In this paper, we investigate the weak lensing effect on the 21cm fluctuations. In order to reconstruct matter density fluctuations along the 21 cm photon path, some authors have been studied the effect (Mandel & Zaldarriaga 2006; Zahn & Zaldarriaga 2006; Metcalf & White 2007; Lu & Pen 2008). For example, Mandel and Zeldarriga studied the effect on the angular power spectra as well as the intrinsic, three-dimensional power spectra of the 21cm fluctuations during the era of reionisation and the effect on both spectra is less than a percent in the interesting scales (Mandel & Zaldarriaga 2006). Metcalf and White studied the lensed shear map power spectrum in 21cm fluctuations and pointed out the potential of producing high resolution, high signal-to-noise images of the cosmic mass distribution (Metcalf & White 2007).

Here we are interested in the two-point correlation function before reionisation. If adopting the Gaussian assumption for the primordial fluctuation field, it is known that the peak statistics can provide additional information about intrinsic distribution of hot spots that those pairs have some characteristic separation angles (Heavens & Sheth 1999). In particular there is a pronounced depression feature in the two-point function around the angular scale of $\theta \sim 40'$ depending on the observed frequency. The weak lensing then redistributes hot spots in the observed 21 cm fluctuation maps from the intrinsic distribution. We found that the effect has large influence in the depression feature, typically several percent contrary to the lensing effect on the power spectra. Moreover, the effect does not very much depend on the details of the nonlinear structure formation. Thus the detailed observation of the redshift dependence of the weak lensing effect as well as of the angular position in the two-point function offer a very useful mean of investigating dark energy equation of state.

This paper is organised as follows. In Sec. II, we calculate and discuss the two-point correlation function of hot spots in the 21 cm line fluctuations. In Sec. III, we give the formalisms the gravitational lensing effect on two-point correlation function. In Sec. IV, we present the result of lensed two-point correlation function and the effect of dark energy equation of state. Finally, we conclude in Sec. V. As the fiducial cosmological model in this paper, we assume the Λ CDM cosmology with cosmological parameters, $h = 0.7$ ($H_0 = h \times 100 \text{ km s}^{-1} \text{ Mpc}^{-1}$), $\Omega_m = 0.3$, $\Omega_\Lambda = 0.7$ and $\sigma_8 = 0.8$.

2 TWO-POINT CORRELATION FUNCTION OF HOT SPOTS IN THE 21 CM LINE FLUCTUATIONS

In the case of the CMB temperature anisotropy, two-point correlation functions of hot spots can be calculated from the angular power spectrum of the CMB temperature anisotropy under the Gaussian assumption (Heavens & Sheth 1999). Since it is a good assumption that the 21 cm fluctuations before the reionisation have a Gaussian statistic, we can calculate two-point correlation functions of hot spots in the 21 cm fluctuations from their angular power spectrum in the same way as in the case of the CMB temperature anisotropy.

2.1 Angular power spectrum of the 21 cm fluctuations

The observed 21 cm fluctuations at $\lambda = 21(1 + z_{\text{obs}})$ cm can be written as (Zaldarriaga et al. 2004)

$$T(\hat{\mathbf{n}}, z_{\text{obs}}) = T_{21}(z_{\text{obs}}) \int_0^{n_0} d\eta W_{21}(\eta_{\text{obs}} - \eta) \psi_{21}(\hat{\mathbf{n}}, \eta), \quad (1)$$

where η is the conformal time, the subscripts obs and 0 mean the values at the redshift z_{obs} and the present time, respectively, and $W_{21}(\eta_{\text{obs}} - \eta)$ is a response function which characterises the bandwidth of an experiment and normalised as $\int_{-\infty}^{\infty} dx W_{21}(x) = 1$. In this paper, we assume that $W_{21}(\eta_{\text{obs}} - \eta)$ is the delta function for simplicity. In Eq. (1), $T_{21}(z)$ is a normalisation constant which is given by

$$T_{21}(z) \simeq 23 \text{ mK} \left(\frac{\Omega_b h^2}{0.02} \right) \left[\left(\frac{0.15}{\Omega_m h^2} \right) \left(\frac{1+z}{10} \right) \right]^{1/2}, \quad (2)$$

and ψ_{21} is the dimensionless brightness temperature written as

$$\psi_{21}(\hat{\mathbf{n}}, \eta) \equiv x_H(\hat{\mathbf{n}}, \eta) [1 + \delta_b(\hat{\mathbf{n}}, \eta)] \left[1 - \frac{T_{\text{cmb}}(\eta)}{T_s(\hat{\mathbf{n}}, \eta)} \right], \quad (3)$$

where δ_b is the baryon density contrast, x_H is the fraction of neutral hydrogen, T_s is the spin temperature of neutral hydrogen and T_{cmb} is the CMB temperature. For simplicity, we assume that the fraction of neutral hydrogen is $x_H = 1$ because the redshifts we are interested in are before the reionisation epoch. We also take another assumption that the gas temperature, T_g , is heated by stars or QSOs, and much higher than T_{cmb} . In this case, T_s is well coupled to T_g and $T_s \gg T_{\text{cmb}}$. As a result, Eq. (3) does not have the dependence on T_s . Under these assumptions, the 21 cm fluctuations are determined only by the baryon density contrast.

Note that the second assumption, $T_s \gg T_g$, might be invalid at high redshifts, if there are not sufficient heat sources to make T_g enough high. In this case, T_s is set by the balance between T_g and T_{cmb} , and the absolute value of the amplitude of the brightness temperature fluctuations depends on T_s (Madau et al. 1997). However, the absolute value of the amplitude does not affect the two-point correlation function in our analysis, since the threshold for a hot spot in this paper is defined relative

to the dispersion of the fluctuations and the correlation function is determined by the gradient and the second derivative of the angular power spectrum as shown in Heavens & Sheth (1999). Therefore, our final conclusion is not significantly changed in the case without the second assumption.

After expanding Eq. (3) in Fourier series and using Rayleigh's formula, we can obtain spherical harmonic coefficients of the 21 cm fluctuations,

$$a_{\ell m}^{21}(z_{\text{obs}}) = 4\pi(-i)^\ell \int \frac{d^3k}{(2\pi)^3} (1 + f\mu^2) \delta_{b\mathbf{k}} \alpha_\ell^{21}(k, z_{\text{obs}}) Y_{\ell m}^*(\mathbf{k}), \quad (4)$$

where $Y_{\ell m}(\mathbf{k})$ is a spherical harmonic function and $\alpha_\ell^{21}(k, z)$ is a transfer function for the 21 cm line,

$$\alpha_\ell^{21}(k, z) \equiv T_{21}(z) D(z) j_\ell[k(\eta_0 - \eta)]. \quad (5)$$

Here, j_ℓ is the spherical Bessel function and $D(z)$ is the linear growth factor of the density fluctuations. We included the factor $(1 + f\mu^2)$ in order to take into account of the redshift-space distortion by the bulk velocity fields, which is called ‘‘Kaiser effect’’, with $\mu \equiv \hat{\mathbf{k}} \cdot \hat{\mathbf{n}}$, and $f \equiv d \ln D / d \ln a$ (Bharadwaj & Ali 2004). The angular power spectrum of the 21 cm fluctuations is obtained from

$$C_{21}(z_{\text{obs}}, \ell) = \langle |a_{\ell m}^{21}(z_{\text{obs}})|^2 \rangle. \quad (6)$$

2.2 Two-point correlation function

For calculating the two-point correlation function of hot spots in the 21 cm line fluctuations, we define the number density fluctuations of hot spots in the 21 cm fluctuation map as

$$\delta n_{\text{pk}}(\theta) = \frac{n_{\text{pk}}(\theta) - \bar{n}_{\text{pk}}}{\bar{n}_{\text{pk}}}, \quad (7)$$

where n_{pk} and \bar{n}_{pk} are the number density and the mean number density of hot spots above a certain threshold ν . The threshold ν is written as $\nu = \Delta T_{21} / \sigma_{21}$ with the 21 cm fluctuations ΔT_{21} and their dispersion,

$$\sigma_{21} \equiv \langle |\Delta T_{21}|^2 \rangle = \frac{1}{(2\pi)^2} \int d\ell^2 C_{21}(\ell). \quad (8)$$

In what follows, we set $\nu = 1$ as the threshold.

The two-point correlation function of hot spots is the ensemble average of the number density fluctuations,

$$\xi_{\text{pk-pk}}(\theta) \equiv \langle \delta n(\boldsymbol{\theta}_1) \delta n(\boldsymbol{\theta}_2) \rangle, \quad (9)$$

where $|\boldsymbol{\theta}_1 - \boldsymbol{\theta}_2| = \theta$. The detailed calculation of the correlation function of hot spots from the angular spectrum is written in Heavens & Sheth (1999). Therefore, we do not give the detailed calculation and we only show some results here.

The left panel in Fig. 1 shows the two-point correlation functions of hot spots in the 21 cm fluctuations. In this figure, we set $z_{\text{obs}} = 30$. The baryonic oscillation brings the oscillatory feature between 20 and 50 arcmin in the correlation function. Since the 21 cm fluctuations do not have Silk damping, the correlation function does not damp below 10 arcmin unlike that of the CMB temperature anisotropy.

Varying the observational wavelength, we can obtain two-point correlation functions at different z_{obs} . We plot the correlation function for different z_{obs} in the right panel of Fig. 1. When z_{obs} are varied from high to low redshifts, the position of the oscillation shifts to large angle. This is because the apparent angular diameter of the baryonic oscillation becomes large at low redshifts. In addition, decreasing the amplitude of the oscillation at low redshifts is also explained by the apparent angular diameter. The increment of the apparent angular diameter makes the baryonic oscillation smooth in the angular power spectrum of the 21 cm fluctuations. Since the two-point correlation function are related to the gradient and second derivative of the angular power spectrum, the smoothing of the baryonic oscillation in low z_{obs} decreases the amplitude of the two-point correlation function.

3 GRAVITATIONAL LENSING EFFECT ON TWO-POINT CORRELATION FUNCTIONS

During traveling to an observer, 21 cm photons are deflected by the gravitational potential of the density fluctuations along the path as CMB photons. Therefore, we measure the lensed 21 cm fluctuations. This means that the number density of hot spots at the direction θ on the observation map corresponds to that at $\theta + \delta\theta$ on the source plane, where $\delta\theta$ is the deflection angle generated by the weak gravitational lensing effect. Therefore, the observed number density fluctuations of hot spots, $\delta n_{\text{pk}}^{\text{obs}}$, are represented as

$$\delta n_{\text{pk}}^{\text{obs}}(\theta) = \delta n(z, \theta + \delta\theta). \quad (10)$$

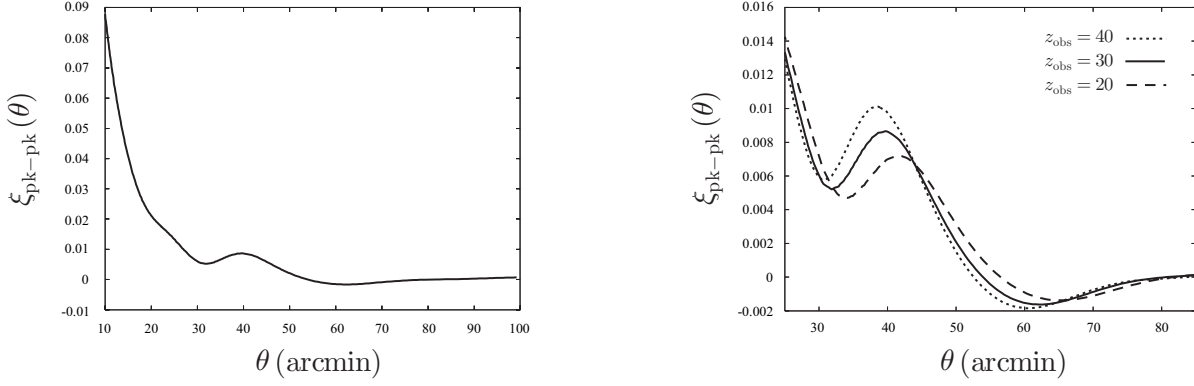


Figure 1. (*Left*) The two-point correlation function of hot spots in the 21 cm fluctuations. We set $\nu = 1$, and $z_{\text{obs}} = 30$. (*Right*) The correlation function for different z_{obs} . The dotted, solid and dashed lines represent the correlation functions for $z_{\text{obs}} = 40$, $z_{\text{obs}} = 30$ and $z_{\text{obs}} = 20$, respectively.

where $\delta n(z, \theta)$ denote the number density fluctuations of hot spots at the redshift z .

The dispersion of $\delta\theta$ for the angular separation θ is written as (Seljak 1996)

$$\sigma_{\text{GL}}^2(\theta) \equiv 2^{-1} \langle |\delta\theta_1 - \delta\theta_2|^2 \rangle = \sigma_{\text{GL},0}^2(\theta) + \sigma_{\text{GL},2}^2(\theta), \quad (11)$$

where $|\theta_1 - \theta_2| = \theta$ and $\langle \rangle$ denotes the ensemble average. In Eq. (11), $\sigma_{\text{GL},0}$ and $\sigma_{\text{GL},2}$ are the isotropic and anisotropic contributions to the lensing dispersion, respectively, and given by

$$\begin{aligned} \sigma_{\text{GL},0}^2(\theta) &= \frac{1}{2\pi} \int \frac{d\ell}{\ell} C_{\text{GL}}(\ell) [1 - J_0(\ell\theta)], \\ \sigma_{\text{GL},2}^2(\theta) &= \frac{1}{2\pi} \int \frac{d\ell}{\ell} C_{\text{GL}}(\ell) J_2(\ell\theta), \end{aligned} \quad (12)$$

Here, $C_{\text{GL}}(\ell)$ is the angular power spectrum of the deflection angle,

$$C_{\text{GL}}(\ell) = 9H_0^4 \Omega_m^2 \int_{\eta_0}^{\eta_{\text{obs}}} d\eta a^{-2}(\eta) W^2(\eta, \eta_{\text{obs}}) P_m \left(k = \frac{\ell}{\chi(\eta)}, \eta \right). \quad (13)$$

where P_m is the matter density power spectrum and $W(\eta, \eta_{\text{obs}})$ is represented as $W(\eta, \eta_{\text{obs}}) = \chi(\eta - \eta_{\text{obs}}) / \chi(\eta_{\text{obs}})$ where χ is the comoving angular diameter distance.

The effect of weak gravitational lensing on the correlation functions of hot spots was investigated by Takada et al. (2000) (see also Takada & Futamase 2001). The lensed two-point correlation function is expressed with the dispersions of the deflection angle as

$$\begin{aligned} \xi_{\text{pk-pk}}^{\text{obs}}(\theta) &= \langle \delta n^{\text{obs}}(\theta_1) \delta n^{\text{obs}}(\theta_2) \rangle_{|\theta_1 - \theta_2| = \theta} = \langle \delta n(\theta_1 + \delta\theta_1) \delta n(\theta_2 + \delta\theta_2) \rangle_{|\theta_1 - \theta_2| = \theta} \\ &= \int \frac{d^2\ell}{(2\pi)^2} \frac{d^2\ell'}{(2\pi)^2} e^{i(\ell \cdot \theta_1 - \ell' \cdot \theta_2)} \langle \delta n_{\ell_1} n_{\ell_2} \rangle \langle e^{i(\ell \cdot \delta\theta_1 - \ell' \cdot \delta\theta_2)} \rangle \\ &= \int_0^\infty \frac{\ell d\ell}{2\pi} C_{\text{pk-pk}}(\ell) \left[\left(1 - \frac{\ell^2}{2} \sigma_{\text{GL},0}^2(\theta) \right) J_0(\ell\theta) + \frac{\ell^2}{2} \sigma_{\text{GL},2}^2(\theta) J_2(\ell\theta) \right], \end{aligned} \quad (14)$$

where, in order to obtain the final expression, we used the Gaussian assumption of δn_{ℓ} ,

$$\langle \delta n_{\ell} \delta n_{\ell'} \rangle = (2\pi)^2 C_{\text{pk-pk}}(\ell) \delta^2(\ell - \ell'), \quad (15)$$

and the following approximation,

$$\langle e^{i\ell \cdot (\delta\theta_1 - \delta\theta_2)} \rangle_{|\theta_1 - \theta_2| = \theta} \simeq 1 - \frac{\ell^2}{2} [\sigma_{\text{GL},0}^2(\theta) + \cos(2\varphi_l) \sigma_{\text{GL},2}^2(\theta)]. \quad (16)$$

The angular spectrum of the unlensed correlation function of hot spots $C_{\text{pk-pk}}$ in Eq. (14) can be related with the unlensed correlation function $\xi_{\text{pk-pk}}^{\text{unlensed}}(\theta)$ as

$$C_{\text{pk-pk}}(\ell) = 2\pi \int_0^\pi d\theta \theta \xi_{\text{pk-pk}}^{\text{unlensed}}(\theta) J_0(\ell\theta). \quad (17)$$

4 WEAK LENSING AND DARK ENERGY

First, we calculate the weak gravitational lensing effect on two-point correlation functions in the fiducial cosmological model. The left panel in Fig. 2 shows the lensed and the unlensed two point correlation functions. The effect of weak gravitational lensing is smoothing of the oscillatory feature of two-point correlation function as in the CMB case (Takada et al. 2000; Takada & Futamase 2001). Therefore, the effect of gravitational lensing arises prominently around 30-50 arcmin where there are the top and bottom of the oscillatory features.

In this calculation, we have not taken into account the nonlinear evolution of matter density fluctuations, although this gives the amplification of gravitational lensing on small scales in the CMB case (Seljak 1996). As shown in Fig. 2, the scale where the gravitational lensing effect arises prominently is about more than 30 arcmin. According to Eq. (12), most contribution of the gravitational lensing effect at each θ comes from $C_{GL}(\ell)$ where ℓ corresponds to $\ell \sim \pi/\theta$. Therefore, the gravitational lensing effect at about 30 arcmin is sensitive to $C_{GL}(\ell)$ at $\ell \sim 300$. The discrepancy between the linear and nonlinear density power spectra on the power spectra of the deflection angle is made on small scales $\ell > 1000$ (see Fig. 1 in Mandel & Zaldarriaga 2006). Thus, neglecting the nonlinear evolution is valid in this paper.

Next, we study the effect of the dark energy equation of state w on weak gravitational lensing in the two-point correlation function. Fig. 3 shows the lensed two-point correlation function for different w . One of the effects of w is the shift of the position of the oscillatory feature in the unlensed correlation function. Decreasing w means that the acceleration of the universe in the dark energy dominated epoch becomes high and the distance to z_{obs} increases. As a result, the oscillatory feature in the correlation function shifts to small angle scale as in the case of the baryonic oscillation in CMB or galaxy redshift surveys (Blake & Glazebrook 2003). Gravitational lensing does not affect the position of the oscillatory feature. Therefore, even in lensed correlation functions, the w -dependence of the position of the oscillatory feature is same as in the case of unlensed correlation functions.

Varying the observational wavelength, we can obtain two-point correlation functions at different z_{obs} . The left panel of Fig. 4 shows the evolution of the position of the oscillatory trough at the redshift z_{obs} for different w . As z_{obs} decreases, the apparent angle of the baryonic acoustic oscillation becomes large. Therefore, the position of the oscillatory trough shifts to large scale with z_{obs} decreasing.

We present the evolution of the fractional change by gravitational lensing at the trough $\Delta\xi/\xi_{\text{pk-pk}}^{\text{unlensed}}$ with $\Delta\xi = (\xi_{\text{pk-pk}}^{\text{obs}} - \xi_{\text{pk-pk}}^{\text{unlensed}})$, as a function of z_{obs} for different w in the right panel of Fig. 4. The deflection angle depends on the distance to the redshift z_{obs} which is the redshift of a ‘source plane’, as described in Eq. (13). Decreasing z_{obs} means that the distance becomes short and the deflection angle by gravitational lensing decreases. Therefore, the integrated value of Eq. (13) is smaller for low z_{obs} than for high z_{obs} .

The amplitude of $\Delta\xi/\xi_{\text{pk-pk}}^{\text{unlensed}}$ depends on w as shown in the right panel of Fig. 4. Decreasing w with keeping z_{obs} makes the comoving distance to z_{obs} large. As a result, integral range of Eq. (13) become large and the gravitational lensing effect is enhanced for small w . The modification of the growth rate of density fluctuations by the dark energy equation of state affects weak gravitational lensing. However we found that this effect is minor in our parameter region ($-1.2 < w < -0.8$), compared with the effect of the modification of the distance to z_{obs} .

At the last, we investigate which redshift makes the most contribution to the lensing effect. Since the gravitational lensing effect mainly arises at about 30 arcmin in the 21 cm fluctuations between $z_{\text{obs}} = 20$ and 40, the dominant contribution to the lensing dispersion in Eq. (12) comes from $C_{GL}(\ell)$ at $\ell \sim 300$. We plot the redshift distribution of $C_{GL}(\ell)$ at $\ell = 300$ in Fig. 5. Varying z_{obs} does not make the distribution change radically, because the radial distances to the source plane at each z_{obs} are not different strongly. For all z_{obs} , the distribution has a peak around $z \sim 1.5$. Therefore, gravitational lensing effect on the 21 cm fluctuations is sensitive to the matter density fluctuations at this redshift

5 CONCLUSION

We have calculated two-point correlation functions of hot spots in 21 cm fluctuations and studied the weak gravitational lensing effect on the correlation function. Particularly, we have examined its possibility as a probe of the equation of state of dark energy w .

The two-point correlation function of hot spots in the 21 cm fluctuations is more smoothed than that of the CMB temperature anisotropy. On large scales, the correlation function is very flat. However, the amplitude of the correlation function increases toward small scales due to the absence of Silk damping in the 21 cm fluctuations. The baryonic acoustic oscillation produces the oscillatory feature around 30-50 arcmin. By decreasing the observation redshift z_{obs} , the oscillatory feature shifts to large scales. Therefore, the position of the oscillatory feature in multi-frequency observations plays a important role in the decision of the cosmological parameter as the baryonic oscillation in the CMB temperature anisotropies and large scale structures.

The weak gravitational lensing effect on the two-point correlation function appears on the oscillatory feature. The effect is smoothing of the feature by smearing the baryonic oscillation without shifting its position. The advantage of the 21 cm

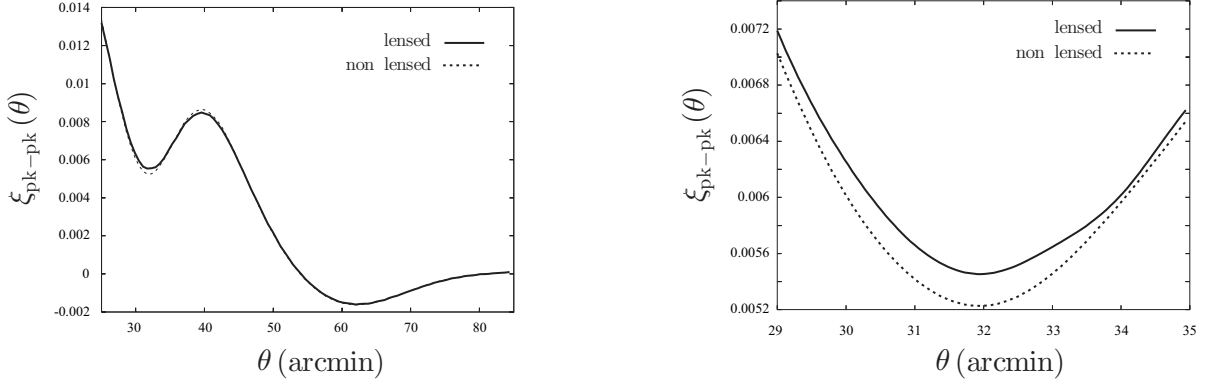


Figure 2. The two-point correlation functions of hot spots in the 21 cm fluctuations. In the left panel, the solid line represents the lensed correlation function and the dotted line indicates the unlensed correlation function. We set $z_{\text{obs}} = 30$ and $\sigma_8 = 0.8$. The right panel shows the result around 30 arcmin in the same case.

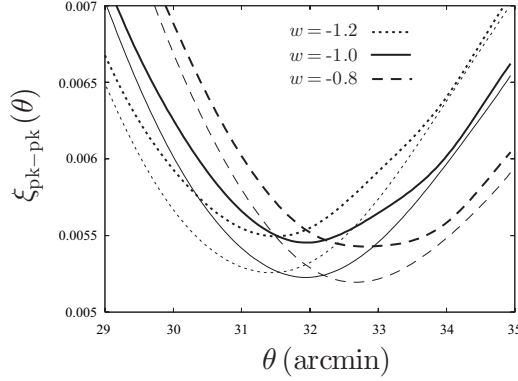


Figure 3. The lensed two-point correlation functions of hot spots for different w . The dotted, solid, and dashed lines represent the lensed correlation functions for $w = -1.2$, $w = -1.0$, and $w = -0.8$, respectively. For comparison, we also plot unlensed correlation function as the thin lines. We set $z_{\text{obs}} = 30$ and $\sigma_8 = 0.8$.

fluctuation observation is that we can obtain independent lensed maps at different redshifts. As z_{obs} decreases, the distance to the source plane becomes small and the deflection angle by gravitational lensing decreases. As a result, the difference between the lensed and the unlensed correlation functions becomes small at low z_{obs} .

We have studied the sensitivity of the 21 cm two point correlation function to the dark energy equation of state w . The effects of w on the two point correlation function appear on the shift of the position of the oscillatory features and the smoothing by gravitational lensing. Since the distance to z_{obs} depends on w , decreasing w makes the position shift to small scale and the smoothing emphasised.

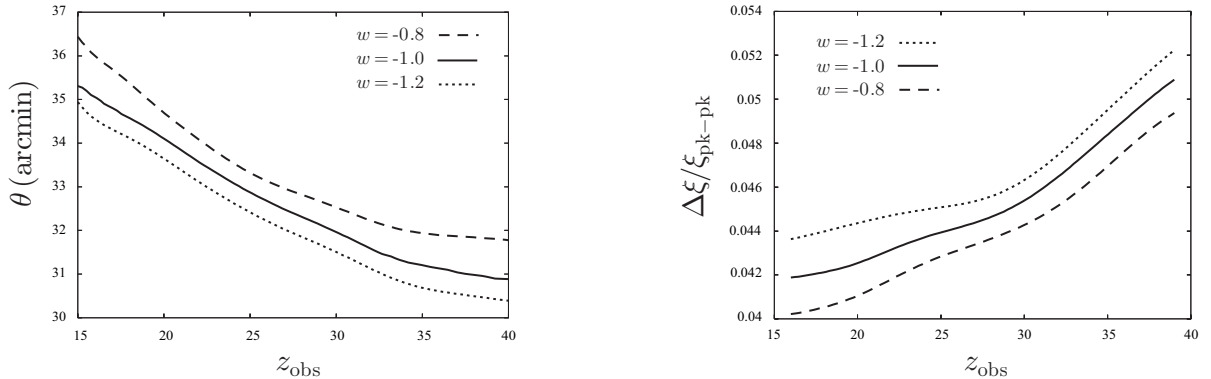


Figure 4. (Left) The evolution of the position of the oscillatory trough for different w . The dotted, solid, and dashed lines are for $w = -1.2$, $w = -1.0$, and $w = -0.8$, respectively. (Right) The evolution of fractional changes of the two-point correlation function for different w . The dotted, solid, and dashed lines represent the evolutions for $w = -1.2$, $w = -1.0$, and $w = -0.8$, respectively.

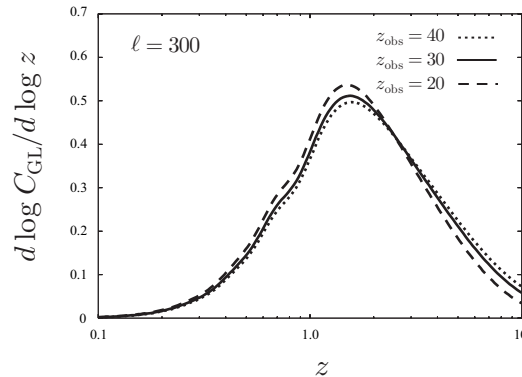


Figure 5. The redshift distribution of $C_{\text{GL}}(\ell)$ at $\ell = 300$ as a function of z_{obs} . The dotted, solid and dashed lines are for $z_{\text{obs}} = 40$, $z_{\text{obs}} = 30$ and $z_{\text{obs}} = 20$, respectively.

The evolution of the fractional change by the gravitational lensing effect, which is obtained from observations of different redshift slices, is useful for the constraint on w . The 21 cm fluctuations with gravitational effect can be estimated from the linear theory. Thus, it will be easy to compare these results with observational data and to obtain the constraint on w .

We mention the comparison between the angular power spectrum and the two-point correlation function of the 21 cm fluctuations for the detection of the gravitational lensing effect. According to Mandel & Zaldarriaga (2006), the fractional change by gravitational lensing in the angular power spectrum is about 1 %. On the contrary, the fractional change is enhanced to about 4 % in the correlation function. Therefore, the two-point correlation function is a better probe of the gravitational lensing effect than the angular power spectrum.

Finally, we give some comments on observational aspects. In this paper, we focus on weak gravitational lensing on the 21 cm fluctuations before the reionisation epoch ($z_{\text{obs}} > 15$). Therefore, we neglect any effect of reionisation process on the 21 cm fluctuations. Planned observational projects in the near future are aimed at the measurement of the 21 cm fluctuations during reionisation ($z_{\text{obs}} \sim 10$ for LOFAR and $z_{\text{obs}} \sim 15$ for SKA). The 21 cm fluctuations from the reionisation epoch are studied with numerical simulations by many authors. The angular power spectrum of the 21 cm fluctuations depends on the reionisation process, (e.g. Baek et al. 2008). Therefore, in order to measure w by the weak gravitational lensing effect in the near future observations, we must take into account the reionisation process precisely with numerical simulations.

REFERENCES

- Adshead P. J., Furlanetto S. R., 2008, *MNRAS*, 384, 291
 Alvarez M. A., Komatsu E., Doré O., Shapiro P. R., 2006, *Astrophys. J.*, 647, 840
 Baek S., Di Matteo P., Semelin B., Combes F., Revaz Y., 2008, arXiv:0808.0925
 Barkana R., Loeb A., 2005, *MNRAS*, 363, L36
 Bharadwaj S., Ali S. S., 2004, *MNRAS*, 352, 142
 Blake C., Glazebrook K., 2003, *Astrophys. J.*, 594, 665
 Heavens A. F., Sheth R. K., 1999, *MNRAS*, 310, 1062
 Lewis A., Challinor A., 2007, *Phys. Rev. D*, 76, 083005
 Lidz A., Zahn O., Furlanetto S. R., McQuinn M., Hernquist L., Zaldarriaga M., 2009, *ApJ*, 690, 252
 Lu T., Pen U.-L., 2008, *MNRAS*, 388, 1819
 Madau P., Meiksin A., Rees M. J., 1997, *Astrophys. J.*, 475, 429
 Mandel K. S., Zaldarriaga M., 2006, *Astrophys. J.*, 647, 719
 Mao X.-C., Wu X.-P., 2008, *Astrophys. J.*, 673, L107
 McQuinn M., Zahn O., Zaldarriaga M., Hernquist L., Furlanetto S. R., 2006, *Astrophys. J.*, 653, 815
 Metcalf R. B., White S. D. M., 2007, *MNRAS*, 381, 447
 Seljak U., 1996, *Astrophys. J.*, 463, 1
 Takada M., Futamase T., 2001, *Astrophys. J.*, 546, 620
 Takada M., Komatsu E., Futamase T., 2000, *Astrophys. J.*, 533, L83
 Tashiro H., Aghanim N., Langer M., Douspis M., Zaroubi S., 2008, *MNRAS*, 389, 469
 Tozzi P., Madau P., Meiksin A., Rees M. J., 2000, *Astrophys. J.*, 528, 597
 Zahn O., Zaldarriaga M., 2006, *Astrophys. J.*, 653, 922
 Zaldarriaga M., Furlanetto S. R., Hernquist L., 2004, *Astrophys. J.*, 608, 622